Human Immunodeficiency Virus Infection of the Human Thymus and Disruption of the Thymic Microenvironment in the SCID-hu Mouse

By Sharilyn K. Stanley,* Joseph M. McCune,‡ Hideto Kaneshima,‡
J. Shawn Justement,* Margery Sullivan,* Elizabeth Boone,*
Michael Baseler,§ Joe Adelsberger,§ Mark Bonyhadi,‡
Jan Orenstein,‖ Cecil H. Fox,¶ and Anthony S. Fauci*

From the *Laboratory of Immunoregulation, National Institute of Allergy and Infectious
Diseases, National Institutes of Health, Bethesda, Maryland 20892; the ‡New Enterprise
Research Division, SyStemix, Inc., Palo Alto, California 94303; the §PRI/DynCorp.,
Frederick, Maryland 21702; the ‖Department of Pathology, George Washington University,
Washington, DC 20037; and the ¶Molecular Histology, Inc., Gaithersburg, Maryland 20879

Summary

Infection with the human immunodeficiency virus (HIV) results in immunosuppression and depletion of circulating CD4$^+$ T cells. Since the thymus is the primary organ in which T cells mature it is of interest to examine the effects of HIV infection in this tissue. HIV infection has been demonstrated in the thymuses of infected individuals and thymocytes have been previously demonstrated to be susceptible to HIV infection both in vivo, using the SCID-hu mouse, and in vitro. The present study sought to determine which subsets of thymocytes were infected in the SCID-hu mouse model and to evaluate HIV-related alterations in the thymic microenvironment. Using two different primary HIV isolates, infection was found in CD4$^+$/CD8$^+$ double positive thymocytes as well as in both the CD4$^+$ and CD8$^+$ single positive subsets of thymocytes. The kinetics of infection and resulting viral burden differed among the three thymocyte subsets and depended on which HIV isolate was used for infection. Thymic epithelial (TE) cells were also shown to endocytose virus and to often contain copious amounts of viral RNA in the cytoplasm by in situ hybridization, although productive infection of these cells could not be definitively shown. Furthermore, degenerating TE cells were observed even without detection of HIV in the degenerating cells. Two striking morphologic patterns of infection were seen, involving either predominantly thymocyte infection and depletion, or TE cell involvement with detectable cytoplasmic viral RNA and/or TE cell toxicity. Thus, a variety of cells in the human thymus is susceptible to HIV infection, and infection with HIV results in a marked disruption of the thymic microenvironment leading to depletion of thymocytes and degeneration of TE cells.

Depletion of mature CD4$^+$ T lymphocytes associated with severe immunosuppression is characteristic of infection with the HIV (1). The mechanism of CD4$^+$ T cell depletion have been postulated to include direct lytic infection by HIV (2); destruction of uninfected cells coated with the soluble viral envelope protein, gp120, by cytotoxic effector cells and antibody-dependent cellular cytotoxicity (3, 4); apoptosis of CD4$^+$ T cells due to abnormal signaling by HIV proteins (5); or autoimmune phenomena (6). HIV infection of either bone marrow or thymic precursor cells leading to their destruction or failure to give rise to more mature progeny could also contribute to peripheral blood CD4$^+$ T cell depletion. In this regard, this laboratory and others (7, 8)

have previously shown that immature thymocyte precursors as well as CD34$^+$ bone marrow progenitor cells (9) can be infected with HIV in vitro. It has also been demonstrated that CD34$^+$ progenitor cells are infected in vivo in some individuals (10) and that human thymocytes can be reproducibly infected with primary isolates of HIV in vivo using the SCID-hu mouse model (11).

Failure to regenerate mature T lymphocytes could also occur if the thymic microenvironment is damaged by HIV infection. Autopsy and biopsy studies have demonstrated that the thymus in HIV-infected individuals is abnormal with effacement of the medulla and cortex, marked involution, and depletion of epithelial elements as well as thymocytes (12–16).

It has been postulated but not demonstrated that the thymic (TE)[1] cell may be a primary target for HIV-induced injury (15).

The SCID-hu xenograft mouse model has been developed as a tool for studying ongoing human thymopoiesis (17, 18, and for a review see reference 19). Mature lymphocytes within the SCID-hu mouse have been shown to be functionally and phenotypically normal (20, 21), and the morphology of the SCID-hu thymus appears similar to the normal human thymus, with distinct medullary and cortical compartments, Hassall's corpuscles, and an appropriate distribution of mature and immature thymocytes (17).

In the present study, the SCID-hu mouse was employed to further delineate the subsets of thymocytes that are susceptible to in vivo infection with HIV and to examine the effects of HIV on the thymic microenvironment. This study demonstrates that both CD4^{+} and CD8^{+} single positive (SP) thymocytes as well as CD4^{+}/CD8^{+} double positive (DP) cells are infected with HIV in the SCID-hu thymus. Furthermore, we demonstrate not only alterations in the microenvironment of the HIV-infected thymus but also the presence of HIV within TE cells.

Materials and Methods

Infection of SCID-hu Mice. The SCID-hu chimeric mice used in this study are C.B-17 *scid/scid* mice into which small pieces (~1 mm³ each) of human second trimester fetal thymus and liver have been implanted under the renal capsule. Over several months, the tissues vascularize, fuse, and mature into a thymic structure that supports ongoing human thymopoiesis (17, 18). SCID-hu mice (SyStemix, Inc., Palo Alto, CA) were used 4–6 mo after implantation of human tissue. To minimize variables, each separate experiment used littermate mice reconstituted with tissue from the same fetal donor. Six different experiments using over 65 mice were performed for this study. Mice were anesthetized and a flank incision made to expose the kidney with the thymic implant. Sterile normal saline or 400–4,000 tissue culture infectious dose$_{50}$ of HIV (in a small volume) was injected directly into the thymus and the flank incision closed. Two different primary HIV viral isolates, the molecularly cloned JR-CSF (22) and the early passage highly cytopathic isolate SM, were used in these experiments. At varying times after infection, individual mice were killed and the human thymus removed. Small pieces of tissue were placed immediately in fixative for immunohistochemistry (IHC), in situ hybridization (ISH), and transmission electron microscopy (TEM). Total thymocytes harvested from the remaining tissue by gentle mechanical dissociation were immediately stained for phenotypic analysis and cell sorting. Because the amount of thymic tissue from which thymocytes were harvested varied according to the initial size of the particular thymus and the amount of tissue taken for histologic studies, variable numbers of thymocytes were obtained from each mouse, so that total thymocyte cell counts were not meaningful when evaluating the effect of infection on thymocyte depletion. However, depletion was evaluated during careful histologic examination of various thymic samples. Additionally, FACS® analysis gives reproducible

results regarding the CD4/CD8 staining pattern of total thymocytes so that preferential depletion of thymocyte subsets could be evaluated.

Fluorescence Activated Cell Sorting and Analysis. Total thymocytes were incubated on ice with anti-CD4 (anti-Leu 3a + 3b FITC, Becton Dickinson & Co., Mountain View, CA) followed by staining with anti-CD8 (anti-Leu 2a PE, Becton Dickinson & Co.) according to the manufacturer's recommendations. Thymocytes were stained with a nonreactive, isotype-matched mAb for background controls. Labeled thymocytes were sorted using an Epics C flow cytometer (Coulter Corp., Hialeah, FL) equipped with a 5W argon laser with a 488-nm excitation wavelength, and sorting logic was controlled using log red versus log green fluorescence bit map gating. Cell aggregates and debris were eliminated using forward angle light scatter gates. Spectral overlap between cells stained with specific antibody and those incubated with FITC or PE isotype controls was electronically compensated using analog subtraction. Cells were sorted at a rate of ~3,000 cells/second with coincidence abort engaged. Cells were sorted into three fractions: CD4^{+}CD8^{+} DP and CD4^{+}CD8^{-} and CD4^{-}CD8^{+} SP cells. Sorted cells were analyzed for purity using machine parameters identical to those for sorting. In general, the populations were >98% pure with the majority of sorts yielding subsets of 99% purity. Contaminating cells were usually <1% CD4^{-}CD8^{-} double negative (DN) or DP in the SP fractions and CD4^{+} or CD8^{+} SP cells in the DP fraction. Sorted cells were washed and pelleted in PBS and frozen as dry pellets for detection of HIV DNA and RNA by PCR analysis.

RNA and DNA PCR. DNA PCR was performed as previously published (23). Briefly, frozen cell pellets were lysed at a concentration of 10⁵ cells per 50 μl, and DNA from this number of cells analyzed. Primers used were SK38/39 (*gag* 1551–1578/1638–1665) and SK70/JG69 (*env* 7841–7875/7959–7937) (Synthecell Corp., Rockville, MD). Reactions (50 μl of DNA lysate, 50 pmol of each primer, 200 μM each of the four deoxynucleotide triphosphates [Boehringer Mannheim, Indianapolis, IN] 10 mM Tris-HCl, 2.5 mM MgCl₂, 50 mM KCl, 0.2% gelatin, and 2 U Taq polymerase [Perkin-Elmer Cetus, Norwalk, CT] in 100 μl total volume) were run for 31 cycles of denaturation (94°C), annealing (55°C), and extension (72°C). Amplified products were detected by liquid hybridization to ³²P-labeled ATP end-labeled probes (SK 19 [*gag* 1595–1635] or SK69 [*env* 7922–7942], respectively) and analyzed on 10% polyacrylamide gels followed by exposure to film (Eastman Kodak Co., Rochester, NY) for varying lengths of time. For quantification of viral burden, serial dilutions of the lysed sample DNA were added to DNA from 10⁵ Jurkat cells and amplified as described. Signals on autoradiography were compared with those from simultaneously run dilutions of ACH-2 cells, a chronically infected T cell line that contains one provirus per cell, as previously described (24).

RNA PCR was performed according to the method of Graziosi et al. (25). Briefly, RNA was isolated from frozen cell pellets using the RNAzol method (Tel-Test, Inc., Friendswood, TX) followed by isopropanol and then ethanol precipitations. Samples were then treated with DNase (Boehringer Mannheim) at room temperature for 1 h with frequent vortexing, followed by heat inactivation of the DNase and immediate use of the samples in the PCR reaction. Reverse transcription and cDNA amplification were carried out in the same reaction mixture without addition of reagents between reactions, so that reverse transcription was directed by the antisense primer. The reaction mixture differed from that for DNA PCR only in that primers were used at 250 pmol each and 25–30 U AMV reverse transcriptase (RT; Life Sciences, Inc., St. Petersburg, FL) were added initially to each reaction. Reverse transcription was car-

---

[1] *Abbreviations used in this paper:* DN, double negative; DP, double positive; IHC, immunohistochemistry; ISH, in situ hybridization; SP, single positive; TE, thymic epithelial; TEM, transmission electron microscopy; TN, triple negative.

ried out for 10 min at 42°C followed by amplification using the same parameters as those used for DNA PCR for 35 cycles. Reaction products were analyzed as for DNA PCR. SK38/39 primers with the SK19 probe were used to detect unspliced *gag* RNA and the TR-5/TR-3 (5953–5974/8414–8395) primer pair with the TR-4 probe (5975–5999) used to detect spliced mRNA for the *tat/rev* messages. With each experiment, RNA was extracted in parallel from 8E5 cells, a chronically HIV-infected T cell line that constitutively expresses HIV (26). The isolated RNA was divided into two equal portions each representing the RNA derived from 1,000 cells and run either with or without the addition of the RT enzyme to serve as positive and negative controls.

In Situ Hybridization/Immunohistochemistry. ISH/IHC was performed by a procedure described at length elsewhere (27). Briefly, silanized slides were deparaffinized, acetylated, and hybridized with a truncated HIV probe representing all of the HIV-1 genome. After hybridization, the slides were exhaustively washed, digested with RNase, and coated with Kodak NTB3 emulsion. After 4-d exposure, the slides were developed and stained with hematoxylin. Combined ISH/IHC stains were performed using the method described by Spiegel et al. (28). Lymphocyte mAbs used in this study were obtained from Dako Corp. (Carpinteria, CA), and AE1 and AE3 from Boehringer Mannheim.

TEM. Small pieces (4–8, <1 mm) of thymic explant, fixed, at least overnight, in 2.5% glutaraldehyde (buffered to pH 7.2 with 0.1 M Na cacodylate buffer), were postosmicated, dehydrated in increasing concentrations of ethanol and propylene oxide, and embedded in Spurr's epoxy (29). 1 μm, semi-thin plastic sections were cut with glass knives and stained with methylene blue, azure-II, and basic fuchsin. The sections were analyzed by light microscopy and at least two blocks were selected for ultrastructural study. Thin sections (600 A) were cut with diamond knives, mounted on copper grids, stained with uranyl acetate and lead citrate, and examined on a Zeiss EM 10 operating at 60 kv.

Results

Maturation of the Human Thymus in SCID-hu Mice. SCID-hu mice were harvested at varying times after intrathymic injection of either sterile normal saline or HIV in saline. The typical mock-infected thymic explant had a normal histologic appearance (Fig. 1 *A*), consistent with previous reports (17, 18). Specifically, thymic lobules were present with normal appearing Hassall's corpuscles in the medullary region, and IHC staining for HLA-DR revealed a dense interconnected stromal network most striking in the medulla (Fig. 1 *B*), which is a previously reported normal finding in the human thymus (30). Thus, as demonstrated in these experiments and previously (17, 18), the thymus which develops in the SCID-hu mouse appears to have the major features of normal human thymus.

Histology of the HIV-infected Thymus. An HIV-infected thymus is shown in Fig. 1 *C* and differs markedly from the mock-infected thymus shown in Fig. 1 *A*. The HIV-infected thymic explant has a large fibrous component, more adipose tissue (suggestive of the occurrence of atrophy), less well demarcated cortical/medullary junctions, and varying numbers of preserved Hassall's corpuscles. ISH gives a signal consistent with the presence of large amounts of HIV RNA (Fig. 1 *D*). In contrast to what has been shown previously in the infected hyperplastic lymph node, where much of the RNA

represents extracellular virions attached to processes of follicular dendritic cells (31, 32), the HIV RNA detected in the thymus is most likely intracellular mRNA since the signal does not increase after protease digestion (data not shown). When ISH for HIV was combined with IHC staining for a variety of antigens, it was found that both CD4$^+$ and CD4$^-$ cells were infected with HIV whereas macrophages did not appear to be infected (data not shown).

Two different viral isolates were used in these experiments and varying degrees of thymocyte depletion were observed histologically. Fig. 2 shows several examples of thymuses that were stained for cytokeratins, a pink stain that specifically identifies the TE cell. At 8 wk after infection with the JR-CSF isolate, minimal thymocyte depletion was observed, and the densely packed thymocytes tend to obscure the underlying TE cell network (Fig. 2 *A*). In comparison, Fig. 2 *B* shows a thymus harvested 3 wk after infection with the SM isolate. The diminished number of thymocytes allows one to now readily identify the presence of pink-stained, keratin-containing TE cells in an intricate supporting network. Similar thymocyte depletion was observed in thymuses infected with the JR-CSF isolate at 12 wk after infection with discrete foci of cells staining positively by ISH for HIV RNA clearly visible (data not shown). Some areas of these thymuses contained clearly identified TE cells that were negative by ISH for HIV in the same field as keratin-negative cells stained intensely positive by ISH that were likely thymocytes (Fig. 2 *C*). However, further examination of these thymocyte-depleted tissues also revealed keratin-staining cells that were clearly positive by ISH for intracellular HIV RNA (Fig. 2 *D*). Thus, the use of HIV ISH combined with IHC for a variety of cell-associated antigens resulted in the identification of both CD4$^+$ and CD4$^-$ HIV-infected thymocytes, as well as the detection of TE cells containing HIV RNA.

Evaluation of Viral Burden and Viral Expression in Thymocytes from the SCID-hu Thymus. Because many of the HIV-positive cells on ISH were CD4$^-$ but appeared morphologically to be thymocytes, we determined further which subsets of thymocytes were infected with HIV and the kinetics of this infection. Total thymocytes were harvested from the human thymic implants at progressively longer times after infection and sorted into highly purified SP (CD4$^+$ SP or CD8$^+$ SP) or CD4$^+$/CD8$^+$ DP subsets. Unfractionated total thymocytes were also analyzed. Fig. 3 shows the results of DNA PCR performed on sequentially obtained thymocyte subsets in one representative experiment using the HIV primary isolate JR-CSF for infection. By 1 wk after infection, a positive signal for *gag* DNA can be seen in the unfractionated, CD4$^+$ SP and CD8$^+$ SP subsets whereas the DP cells remain negative. Infection can be detected in the DP cells by the second week, with significant increases in viral burden occurring in all three cell subsets over the following 2 wk (Fig. 3). In this particular experiment, the viral burden in the CD4$^+$ SP subset at 1 wk is equivalent to or only slightly greater than that in the CD8$^+$ SP subset (titration data not shown). However, results from two other experiments using this viral isolate revealed more clearly that the CD4$^+$ SP cells are the initial subset of thymocytes infected,
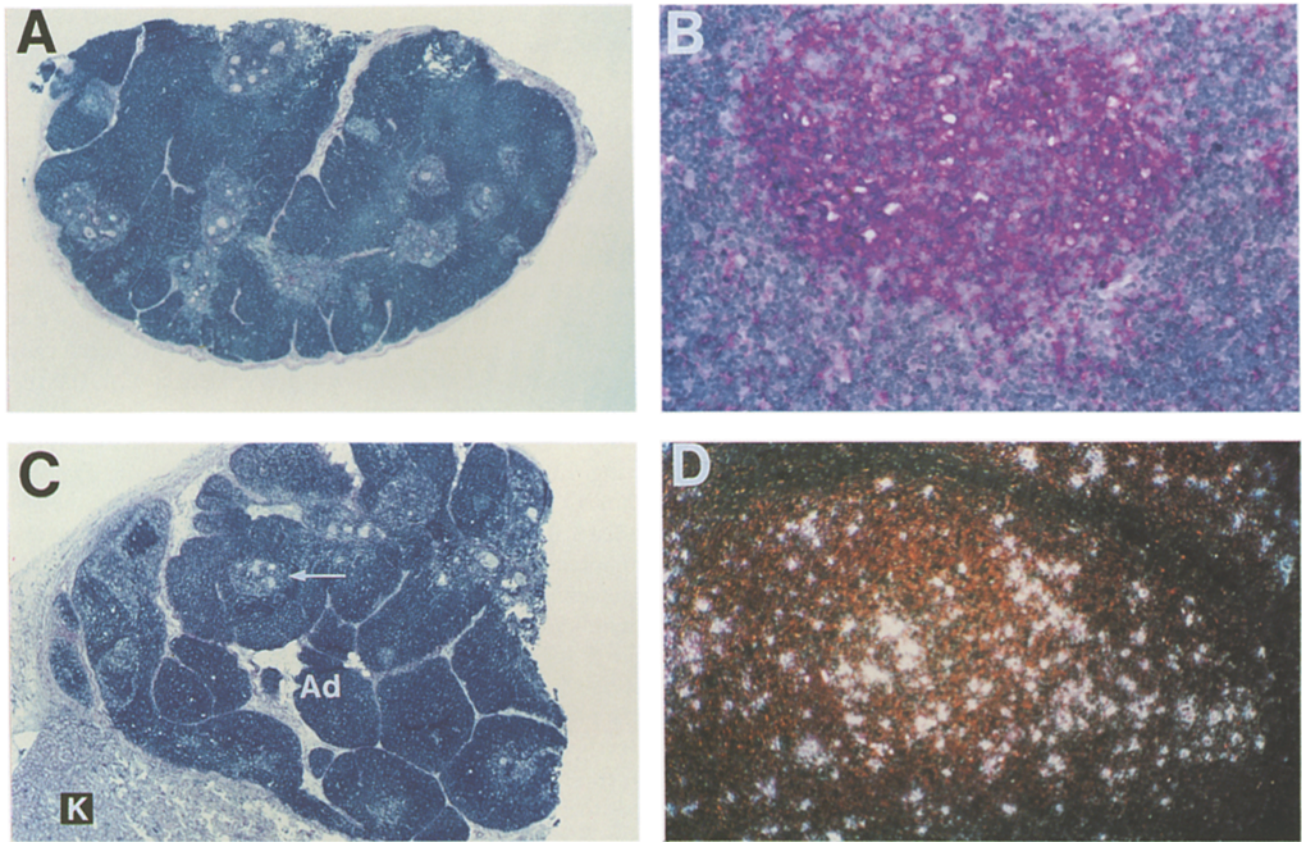
Figure 1. Histology of the mock- and HIV-infected SCID-hu human thymus. (*A*) A typical thymus harvested 2 wk after mock infection and processed as described in Materials and Methods. (×16 magnified Giemsa stain). (*B*) Staining of the mock-infected thymus with anti-HLA-DR reveals a network of DR-positive processes, most prominent in the medulla which contains a lower number of thymocytes. (*C*) A ×20 magnified, Giemsa-stained section of thymus (2 wk after infection with JR-CSF) with fibro-adipose tissue (*Ad*), Hassall's corpuscles (*arrow*), and underlying mouse kidney (*K*). (*D*) Darkfield view of ISH staining for HIV RNA of a 2-wk JR-CSF–infected thymus.

in that a positive DNA PCR signal was seen in only the unfractionated and CD4$^+$ SP subsets at 3 d after infection, with the appearance of virus in the CD8$^+$ SP or the DP cells lagging behind the CD4$^+$ SP cells by 4–10 d. In four separate experiments using the JR-CSF isolate, total viral burden at 8–12 wk after infection, determined by dilutional DNA PCR analysis, varied from 2 to 10% of total thymocytes and from 0.5 to 10% of CD4$^+$ SP, 2 to 10% of CD8$^+$ SP, and 0.5 to 5% of the DP cells. In all four experiments performed thus far with the JR-CSF isolate, viral burden in the CD8$^+$ SP subset equaled or surpassed that of the CD4$^+$ SP subset by 2–4 wk after infection (Fig. 3). Likewise, a consistent finding in all experiments using this isolate is the lower viral burden seen at later time points after infection in the DP thymocytes when compared with either of the SP fractions (Fig. 3). The positive PCR signals seen in the CD8$^+$ thymocyte subset reflects true infection of these cells and could not be due to contamination of the CD8$^+$ cells by infected CD4$^+$ thymocytes, in that the subsets were >98% pure and the intensity of the PCR signals in the two subsets was similar. Indeed, quantitation of viral burden at later time points after infection always revealed an equal or greater burden in the

CD8$^+$ subset when compared with the CD4$^+$ subset, as indicated by a stronger PCR signal on serial dilutional analysis in the CD8$^+$ thymocytes (data not shown).

In contrast with the infection kinetics and viral burden found using the JR-CSF isolate, the more virulent SM isolate displayed an accelerated kinetics of infection, with marked thymocyte depletion occurring by 3 wk after infection, and a higher viral burden in the DP thymocyte subset than in either the CD4$^+$ SP or CD8$^+$ SP cells (viral burden at 3 wk, ∼50% of total thymocytes in two separate experiments, with infection of 50% of the DP and 10% each of the CD4$^+$ and CD8$^+$ SP cells). Additionally, the thymocyte depletion which was so readily observed histologically (Fig. 2) was reflected in a predominant loss of DP and CD4$^+$ SP cells when the SM isolate was used (FACS® analysis of thymocytes from mock thymus revealed 78% DP, 14% CD4$^+$, 7% CD8$^+$, and 1% DN compared to thymocytes from the 3-wk SM-infected thymus which contained 9% DP, 5% CD4$^+$, 58% CD8$^+$, and 28% DN). In contrast, the JR-CSF isolate led to significant depletion of thymocytes much later after infection (week 12) and seemed to cause an overall decrease in all subsets with a significant loss of DP cells (FACS®
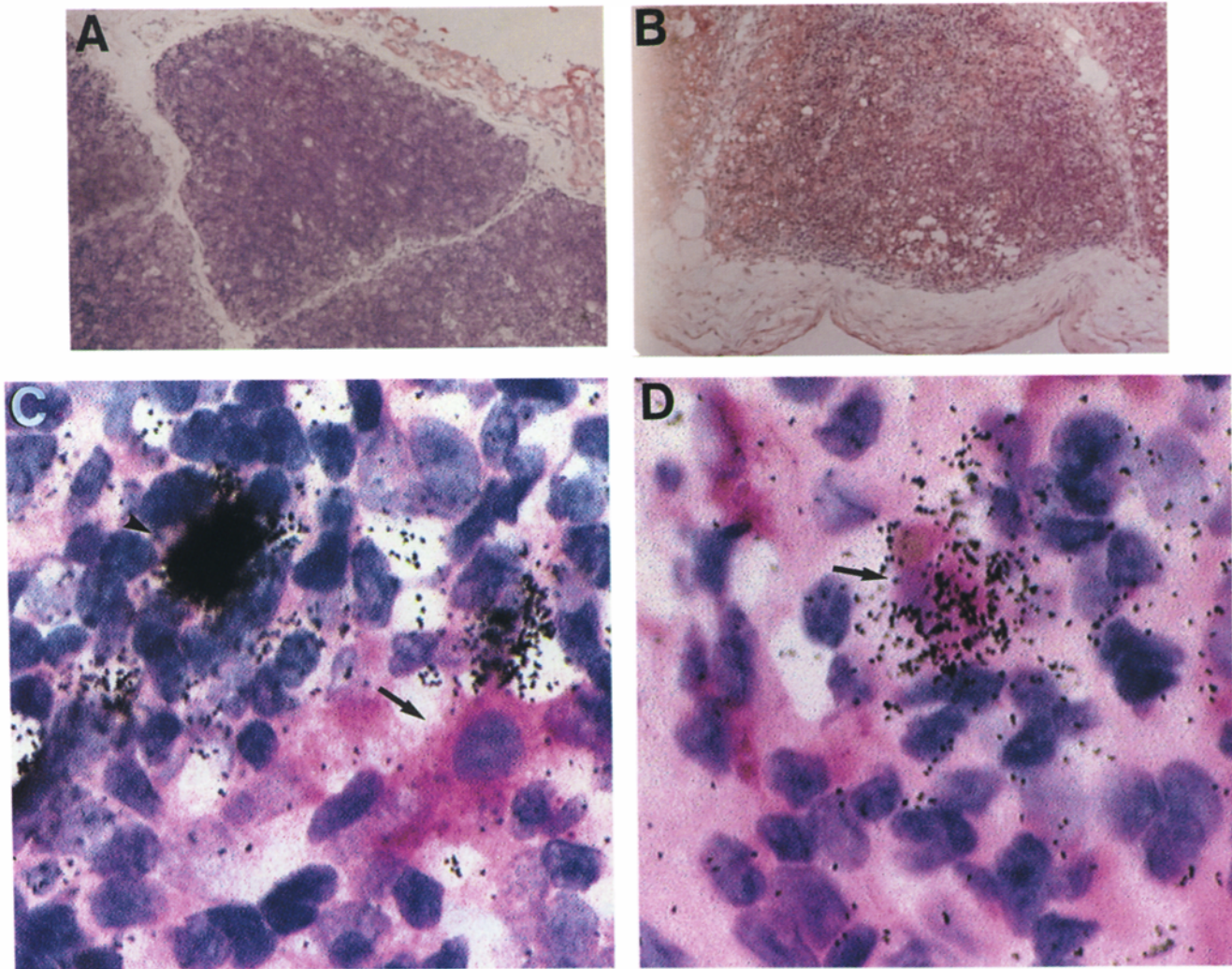
Figure 2. Thymocyte depletion and infection of TE cells. Thymuses from SCID-hu mice were harvested at varying times after infection and examined for HIV RNA by ISH and stained with AE-1 antibody for identification of keratin-containing TE cells. (*A*) Thymus infected for 8 wk with JR-CSF, showing minimal thymocyte depletion. Only faint pink (cytokeratin) staining of TE cells is visible because of overlying thymocytes. (*B*) Thymus infected with SM isolate for 3 wk with marked depletion of thymocytes revealing the underlying TE cell network, stained positively for cytokeratins. (*C*) This 12-wk JR-CSF-infected thymus reveals some thymocyte depletion. A pink-stained, cytokeratin-containing TE cell is clearly seen which is negative for HIV by ISH staining (*arrow*). In contrast, a cell stained intensely positive by ISH, indicating active HIV replication, is seen which does not stain for cytokeratins and is probably a thymocyte (*arrowhead*). (*D*) Thymus infected with JR-CSF for 12 wk reveals a TE cell containing cytokeratins and staining positively for cytoplasmic HIV RNA by ISH (*arrow*).

analysis of thymocytes from mock-infected thymus revealed 82% DP, 12% CD4$^+$, 6% CD8$^+$, and 1% DN compared with analysis of 12-wk JR-CSF–infected thymocytes showing 51% DP, 22% CD4$^+$, 23% CD8$^+$, and 5% DN). These results are consistent with the thymocyte depletion seen by other investigators (33a) using these viral isolates in this model of infection.

To evaluate whether the DNA PCR results indicated a productive HIV infection of these various thymocyte subsets, RNA PCR was performed using primers to detect both structural (*gag*) and spliced (*tat/rev*) RNAs. Fig. 4 is representative of the results from three separate experiments. At day 14 large amounts of *gag* RNA were found in the unfraction-

ated and CD8$^+$ SP cells while there was a lesser amount found in the DP and CD4$^+$ SP fractions. By day 60, *gag* RNA had increased in all thymocyte subsets. These semiquantitative RNA findings paralleled the relative viral burden detected in these four subsets by quantitative DNA PCR performed on duplicate pellets of cells in this experiment (data not shown). Messenger RNA for the spliced *tat/rev* message was also present in large amounts in the unfractionated and CD8$^+$ SP cells at day 60 with smaller amounts present in the DP and CD4$^+$ SP subsets (Fig. 4). In two separate experiments *tat/rev* mRNA was detected in the CD4$^+$ and CD8$^+$ subsets as early as 2 wk after infection, whereas it was first detected 30 d after infection in the DP fraction in

Figure 3

Weeks Post Infection

1 2 4 8 10 12

Unfractionated

CD4+

CD8+

CD4/CD8+

Controls

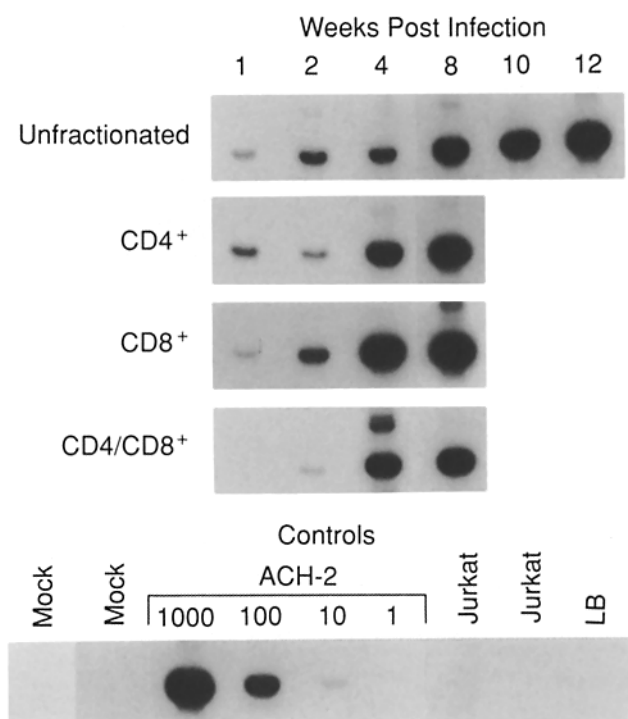Mock   Mock   ACH-2   Jurkat   Jurkat   LB

1000   100   10   1

Figure 3. Increasing viral burden in JR-CSF–infected SCID-hu thymuses. SCID-hu mice were killed at increasing intervals after infection and total thymocytes were harvested, sorted into SP and DP subsets, and analyzed by DNA PCR for the detection of HIV *gag* DNA, as described in Materials and Methods. Results from each thymocyte subset at various times after infection are shown, with positive and negative controls (*bottom panel*). Negative controls consist of mock (total thymocytes from two separate mock infected mice), lysis buffer alone (*LB*), and lysate from the uninfected Jurkat cell line. Positive controls shown are serial dilutions of lysate from the chronically HIV-infected ACH-2 cell line representing DNA from 1,000, 100, 10, and 1 cells. Results are representative of four separate experiments involving infection with the JR-CSF isolate.

Figure 4

Unfractionated   CD4+   CD8+   CD4+ CD8+   Uninfected

d14, GAG

d60, GAG

d60, TAT/REV

GAG   TAT/REV
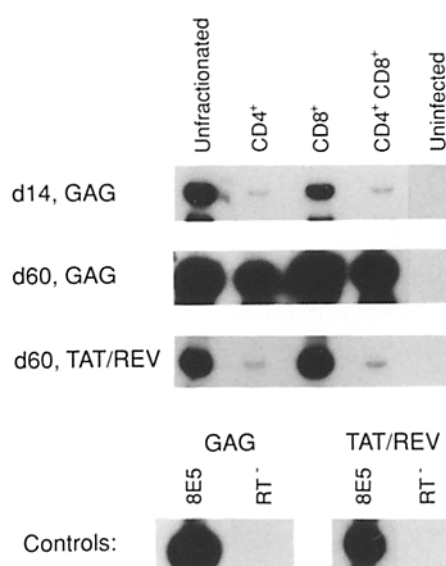
8E5   RT⁻   8E5   RT⁻

Controls:

Figure 4. Productive infection of thymocyte subsets with expression of both spliced and unspliced messages. RNA PCR was performed on RNA extracted from thymocyte subsets harvested and sorted at varying times after infection with JR-CSF, as described in Materials and Methods. Data shown are from a different experiment than that in Fig. 3, and are representative of RNA results obtained from three separate experiments. The results of RNA-PCR analysis are shown using total RNA harvested from the following numbers of available cells: (*d14*) 10^6 unfractionated, DP, and uninfected, and 5×10^5 CD4+ and CD8+ SP; (*d60*) 4×10^5 cells in all infected subsets for each primer pair, and 10^6 thymocytes from an uninfected thymus.

one experiment (data not shown). Thus, productive infection, as indicated by the presence of both structural and regulatory viral mRNAs, occurred in all three thymocyte subsets after inoculation of the thymus with HIV.

Morphologic Patterns of HIV Infection of the Thymus. In addition to the evaluation of individual cell types infected with HIV, the histology of the infected thymuses was ultrastructurally examined. In general, two morphologic patterns of HIV infection in the thymic tissue were observed, involving either predominantly thymocyte infection (Figs. 5 and 6, pattern 1) or destruction of TE cells with or without demonstrable virus within the cells (Figs. 7 and 8, pattern 2). Both morphologic patterns could occur in distinct areas of the same individual thymus.

Examples of the first morphologic pattern, in which thymocytes are predominantly affected, are shown in Fig. 5. A multinucleated giant cell is shown in a thymus infected with the SM isolate (Fig. 5 *A*). This cell is productively infected with HIV in that virions were seen budding from the cell surface

(Fig. 5, *inset*). Indeed, when infected thymocytes were detected by TEM they often displayed multiple buds (Fig. 5 *B*) indicating active localized viral replication. This TEM pattern is consistent with the findings on ISH in which labeling of tissue by the HIV-specific probe often indicated foci of individual cells possessing large amounts of HIV RNA (Fig. 1 *D*). Infection of thymocytes in these thymuses ultimately resulted in thymocyte depletion, as is shown strikingly in Fig. 6. Fig. 6 *A* shows a mock-infected thymus in which the elongated desmosome-linked dendritic-like TE cell processes form a supporting stroma that surrounds individual thymocytes. In Fig. 6 *B*, a section of a thymus infected for 3 wk with the SM isolate is shown in which the supporting TE cell stromal network appears to be relatively healthy and intact with preserved junctions between cells, whereas the loss of thymocytes is readily apparent in the abundant spaces left between TE cells. This marked thymocyte depletion was most easily observed by TEM with the rapidly cytopathic SM isolate as compared with the JR-CSF isolate, and occurred as early as 2–3 wk after infection.

The second morphologic pattern observed in the HIV-infected thymuses involved the destruction of the thymic microenvironment, most notably infection and/or depletion of TE cells. A low power TEM view of a cell with morphological features of a TE cell in a thymus infected for 2 wk with JR-CSF is shown in Fig. 7 *C* with higher power views
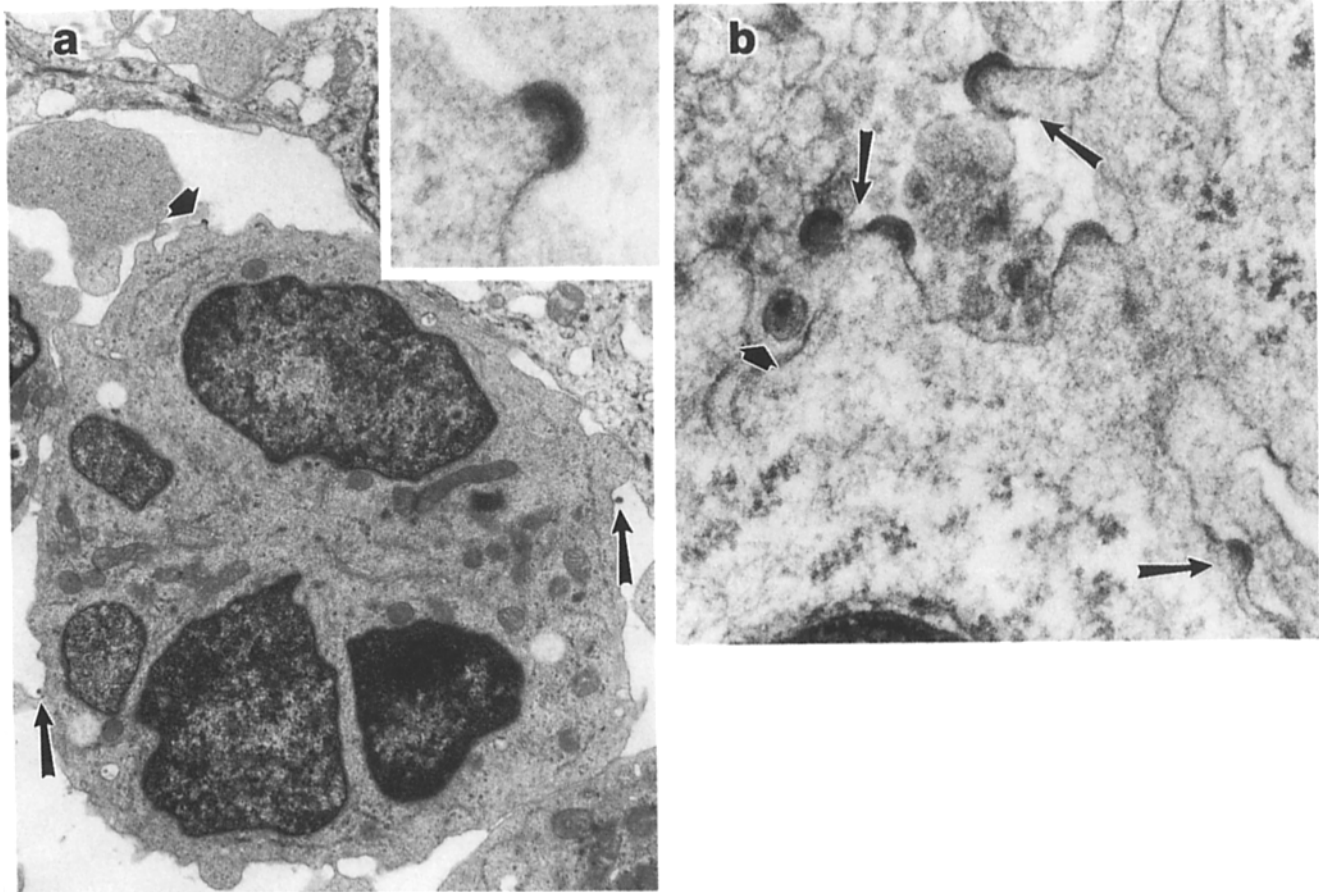
Figure 5. Morphologic pattern of HIV infection in the thymus with predominance of thymocyte involvement (pattern I). Infected thymuses were harvested at varying times after infection with either the SM or JR-CSF isolate of HIV and processed for TEM analysis as described in Materials and Methods. (*A*) A multinucleated thymocyte, in a thymus infected with the SM isolate for 3 wk, with three plasma membrane particles (*long and short arrows*). (×8,000). The inset is a higher magnification of one of the budding particles (*short arrow*). (×110,000). (*B*) A small portion of the surface of a large multinucleated thymocyte in a thymus infected for 2 wk with JR-CSF with mature particles having a conical nucleoid (*short arrow*) and several budding particles (*long arrows*). (×63,000).

of this cell shown in the other panels. Although this cell appears healthy, HIV is present, clustered both extracellularly (Fig. 7 *B*) and in vacuoles within the cell (Fig. 7, *A* and *D*). HIV was observed both in coated vacuoles (Fig. 7 *D*), possibly indicating endocytosis of HIV by TE cells, as well as in multivesicular bodies, a component of the Golgi complex (Fig. 7 *A*). In the examination of multiple thymuses, HIV was frequently seen intimately associated with cells clearly identified as TE cells by the presence of desmosomes and intracellular tonofilaments. These data, in combination with the ISH/IHC data shown in Fig. 2 *D*, indicate that HIV is contained within TE cells in this model of human thymopoiesis, although productive infection of these cells could not be formally demonstrated.

Another feature of the second pattern of morphologic involvement of the thymus after HIV infection is shown in Fig. 8. In this thymus harvested 2 wk after infection with the JR-CSF isolate, no obvious infection of TE cells, thymocytes, or free HIV virions are seen in this microscopic field,

yet marked toxicity to a portion of the TE cells has occurred. Healthy TE cells are seen in the periphery of the field, still attached by junctions to obviously abnormal vacuolated and degenerating TE cells. Despite this TE cell degeneration, the thymocytes within the field appear normal. These morphologic findings are consistent with a toxic insult to these particular TE cells resulting in degeneration of this area of the supporting stromal network.

Thus, one morphologic pattern is that of exuberant viral replication by individual thymocytes, formation of multinucleated giant cells with budding virus, and marked thymocyte depletion. In contrast, a second pattern involves alteration of the thymic microenvironment. In this pattern, TE cells contain HIV and are destroyed, either by HIV itself or by some currently unidentified HIV-associated toxic stimulus. Although both morphologies could be seen in the same thymus, infection with the SM isolate generally resulted in a predominance of thymocyte involvement whereas the JR-CSF isolate led to TE cell involvement and destruction in
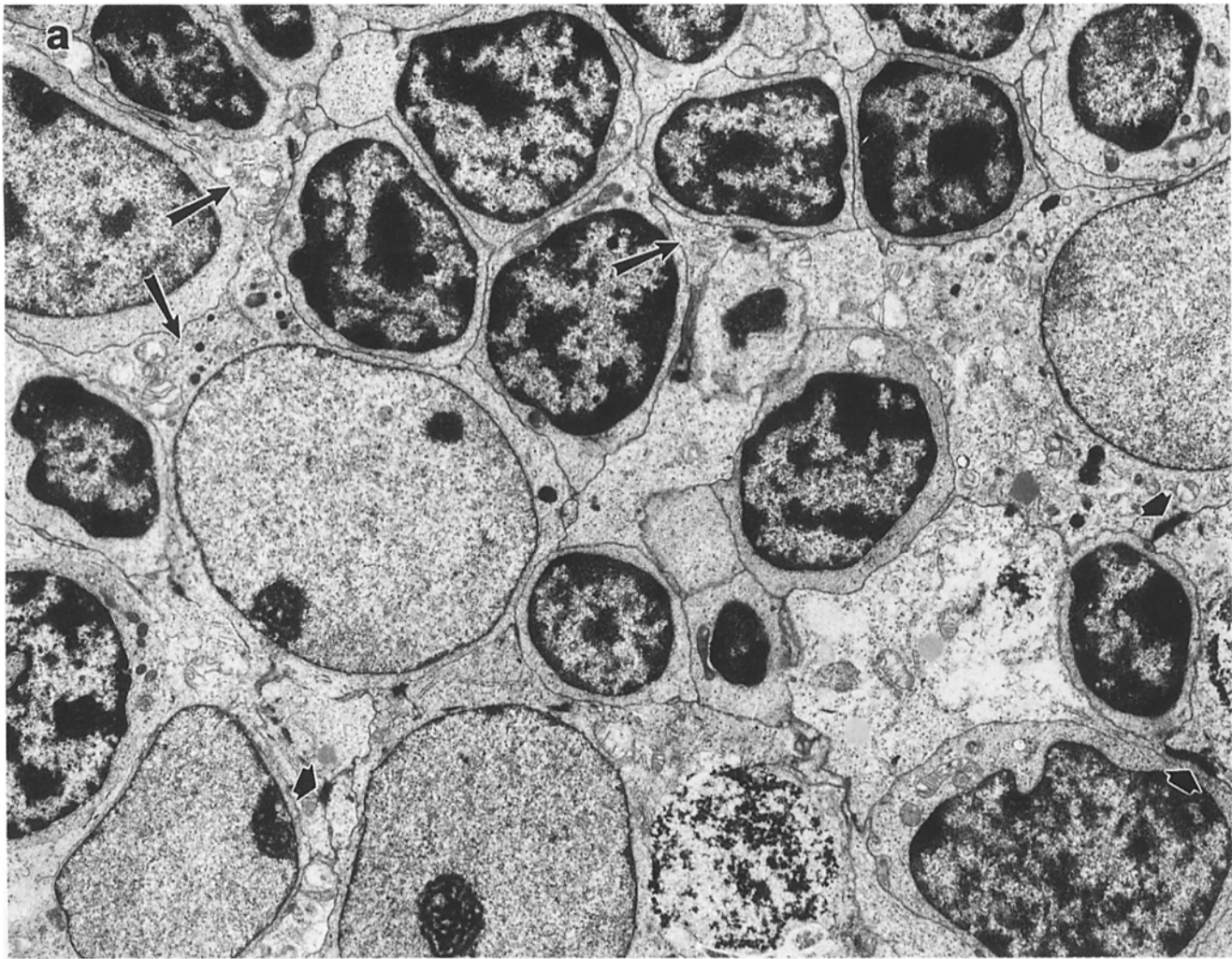
Figure 6. Thymocyte depletion in the HIV-infected thymus compared with the normal thymus. (*A*) TEM of a field from a 2 wk mock-infected explant showing thymocytes intimately associated with the cell bodies and processes (*long arrows*) of four thymic epithelial cells. These TE cells have large nuclei with little heterochromatin and one or two small nucleoli. Many electron-dense desmosomes join TE cells (*short arrows*). (*B*) An area of thymocyte drop-out is shown in a 3 wk SM-infected thymus, in which primarily empty spaces separate TE cells and their many processes. Abundant electron-dense cytokeratin is seen in all of the TE cells (*arrows*). (×5,200).

addition to the thymocyte infection readily detected by PCR analysis.

Discussion

This study demonstrates that intrathymic injection of primary isolates of HIV results in the reproducible infection of multiple subsets of thymocytes as well as the presence of HIV within TE cells, leading to depletion of thymocytes and damage to the thymic microenvironment. Whereas DNA and RNA PCR analyses indicated productive infection of CD4$^+$ and CD8$^+$ SP as well as DP thymocytes, the pattern of infection and viral burden differed both within the three thymocyte subsets and between the two viral isolates used. These findings expand upon previous observations of thymo-

cyte depletion after infection of the SCID-hu mouse with primary isolates of HIV (33).

The reproducible finding of HIV infection within the SP CD8$^+$ thymocytes was surprising. Infection in this subset of cells could reflect infection of DP cells with a resultant decreased surface expression of the CD4 molecule. This seems somewhat unlikely, however, since the viral burden in the DP cells was always significantly less than that seen in the CD8 SP cells (using the JR-CSF isolate), and it is difficult to envision that modulation of the CD4 molecule could occur with such rapid kinetics to give these results. Alternatively, CD8$^+$ cells, particularly more immature cells, may still possess a small amount of CD4 on their surface resulting in susceptibility of these cells to infection by HIV. The subsequent high viral burden observed in this subset might then reflect the balance between a similar susceptibility of CD4$^+$
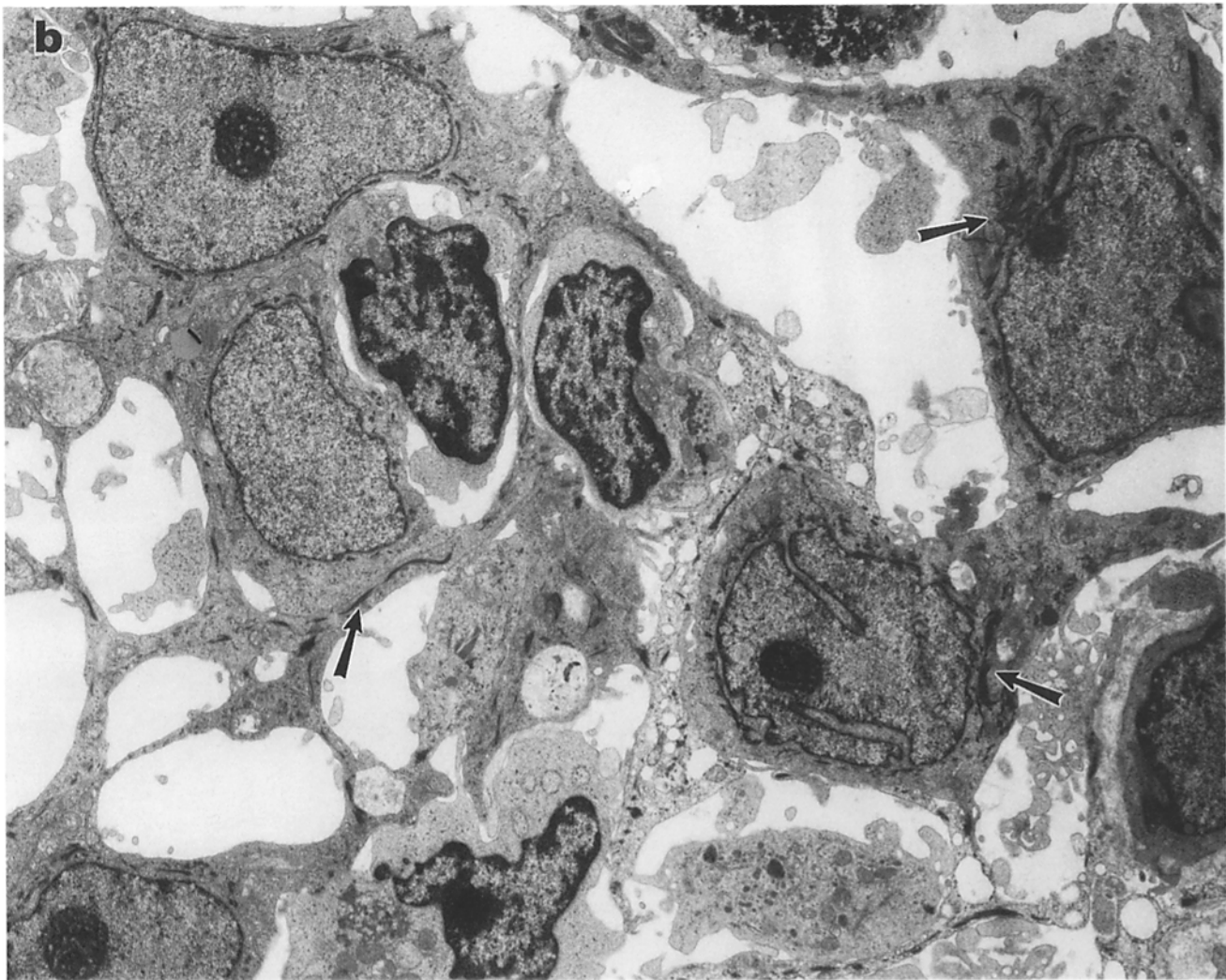
and CD8^{+} SP cells to infection and a lower HIV-induced cytotoxicity for the CD8^{+} cells, since cytotoxicity has previously been positively correlated with levels of expression of CD4 on the surface of an infected cell (34, 35). A third potential explanation is that infection occurs in the so called "triple negative" (TN, CD3^{-}CD4^{-}CD8^{-}) thymic precursor cells, a subset that has been previously demonstrated to be infectable in vitro (7). The infected TN cell might then be preferentially driven to mature along the CD8 SP pathway, resulting in an accumulation of infected CD8^{+} SP cells. Since TN cells comprise an extremely small percentage of the population of thymocytes harvested from these SCID-hu thymuses (cells staining negatively for both CD4 and CD8 generally <1.5% by FACS® analysis, data not shown), it has not been possible thus far to purify these cells for detection of HIV infection. Finally, relatively mature SP CD8^{+} thymocytes could become infected in the thymic microenvironment by a cell–cell mechanism, much like that which has been previously reported to occur after coculture with mature peripheral blood T cells from HIV-infected individ-

uals (36). Whereas circulating mature CD8^{+} cells are not infected with HIV (23), De Maria et al. (36) demonstrated that coculture of mature peripheral blood CD8^{+} T cells with autologous infected CD4^{+} T cells from seropositive individuals resulted in the ability to derive CD8^{+} T cell clones from these cultures which were productively infected with HIV. This in vitro infection was presumably the result of culturing the previously uninfected CD8^{+} T cells with a higher number or concentration of productively infected autologous CD4^{+} cells than that which is seen in the circulation in vivo. In this regard, the close environment of the SCID-hu human thymus may well provide an appropriate milieu such that cell-mediated infection of CD8^{+} SP thymocytes can occur. Since infected CD8^{+} cells are not seen in the peripheral circulation of seropositive individuals, the fate of these cells is uncertain. Whether intrathymic death or tissue sequestration occurs remains an area for further evaluation. Studies are ongoing to delineate whether mature or immature CD8^{+} thymocytes are infected with HIV and to determine the mechanism of this infection and the fate of these cells.
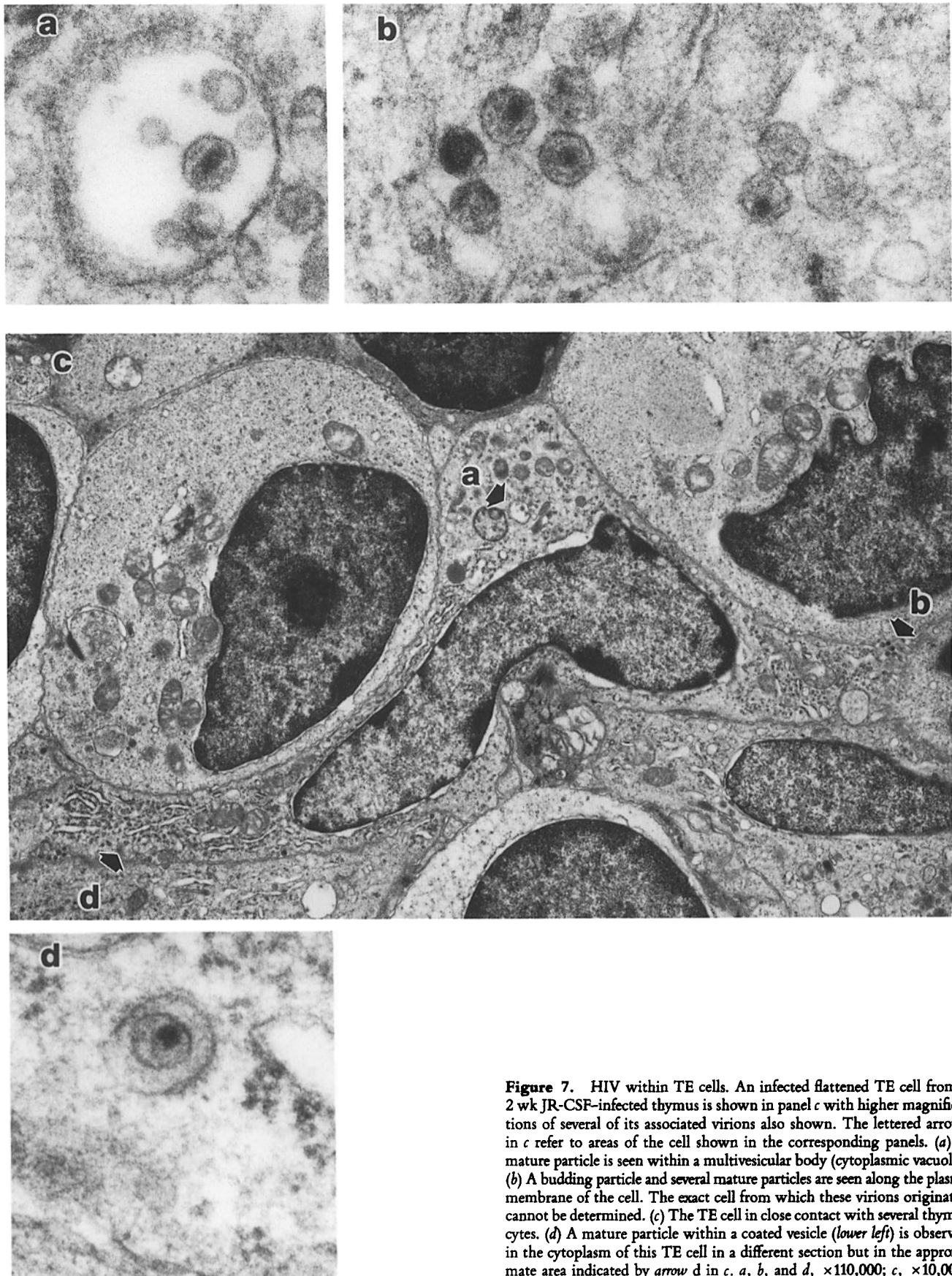
1159   Stanley et al.

Figure 7. HIV within TE cells. An infected flattened TE cell from a 2 wk JR-CSF–infected thymus is shown in panel c with higher magnifications of several of its associated virions also shown. The lettered arrows in c refer to areas of the cell shown in the corresponding panels. (a) A mature particle is seen within a multivesicular body (cytoplasmic vacuole). (b) A budding particle and several mature particles are seen along the plasma membrane of the cell. The exact cell from which these virions originated cannot be determined. (c) The TE cell in close contact with several thymocytes. (d) A mature particle within a coated vesicle (lower left) is observed in the cytoplasm of this TE cell in a different section but in the approximate area indicated by arrow d in c. a, b, and d, ×110,000; c, ×10,000.
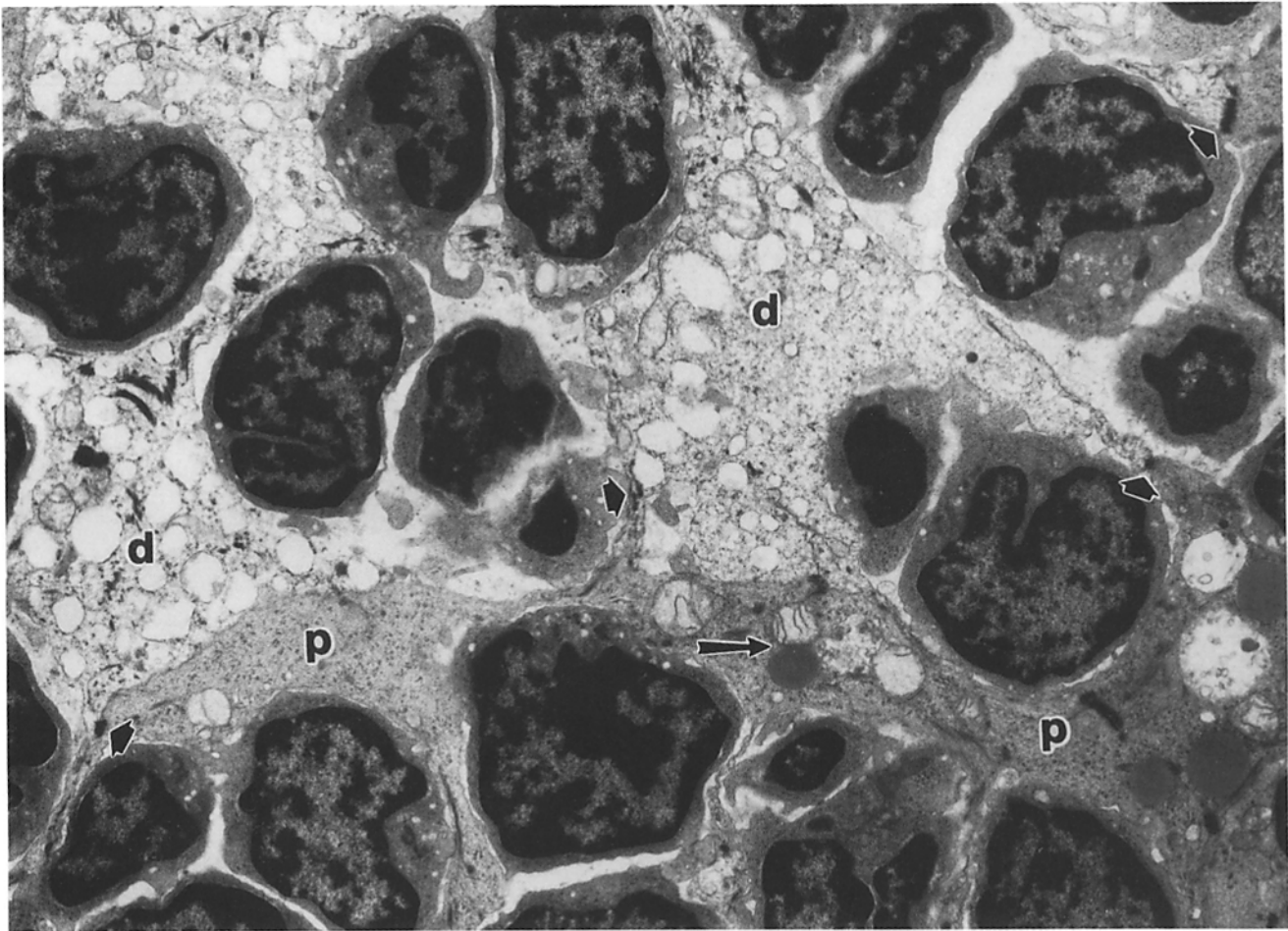
Figure 8. TE cell degeneration in the infected thymus. In this thymus harvested 2 wk after infection with JR-CSF, more normal-appearing TE cell processes (*p*), with occasional swollen mitochondria and electron-dense lipid vacuoles (*long arrow* pointing to mitochondrion touching lipid vacuole) are attached by desmosomes (*short arrows*) to the electron-lucent degenerating TE cells (*d*). No virions are seen in this field. (×6,500).

Involvement of the TE cell in this infected tissue was examined by both TEM and ISH/IHC techniques. IHC/ISH double labeling demonstrated the presence of keratin-containing TE cells stained positively for HIV RNA, whereas TEM examination revealed HIV intracellularly and intimately associated with TE cells, although budding virus could not be definitively shown. In this regard, it is possible that the positive signal seen by ISH in TE cells may reflect the presence of intracellular viral RNA and not mRNA, and the internalization of virus may not result in productive infection of these cells. Nevertheless, the demonstration of intracellular HIV in TE cells in the SCID-hu human thymus is of considerable interest. Previous studies (12–16) have demonstrated that thymuses from HIV-infected individuals are markedly abnormal and display evidence of premature involution and TE cell toxicity. Whereas ISH results obtained by Schuurman et al. (14) were suggestive of TE cell infection, this phenomenon has not been definitively demonstrated in vivo. In vitro infection of cultured TE cells has been accomplished resulting in a transient low level production of p24 and TE cell death by 8–10 d (37), although it is unclear

whether contaminating thymocytes or other cells were present in the initial cultures. Our data indicate that TE cells become infected with HIV in vivo, but the presence of HIV did not seem to correlate with destruction of the TE cell. This difference in TE cell cytopathology could be due to the differences between an in vivo versus an in vitro system. As an example, HLA-DR is constitutively expressed by TE cells in the thymus, whereas cultured TE cells do not express this antigen unless exogenous IFN-γ is added to the media (38). Additionally, there are multiple subtypes of TE cells within the thymus representing different stages of maturation and different functions and containing variable amounts of cytokeratins (30). These can be identified by the expression of antigens that distinguish medullary and subcapsular endocrine functioning TE cells from the cortical TE cells. In fact, as many as six different types of TE cells have been identified ultrastructurally (39). Studies are ongoing to determine whether there are differences in susceptibility to HIV infection among TE cell subsets and to delineate any functional alterations that may occur in these cells. The lack of toxicity noted in TE cells containing HIV (e.g., Fig. 7) might be a

function of the timing of tissue harvest after infection, or may indicate that infection in vivo is chronic, noncytopathic, and nonproductive or associated with low levels of virus production, similar to the pattern of infection observed in tissue macrophages. In this regard, the majority of immature particles seen in these tissues were budding from thymocytes, suggesting that the virus within TE cells is indeed either nonreplicative or associated with only a low level of virus production as compared with thymocytes. This would have significant implications for the potential role of these cells as a viral reservoir in which newly developing and susceptible thymocytes are chronically exposed to HIV. Current studies in this laboratory are addressing these issues.

TE cell toxicity was noted that was seemingly unrelated to productive infection of these cells. One can speculate that infection and destruction of thymocytes could result in their failing to produce TE trophic factors such as IFN-γ or IL-2, resulting in death of the TE cells. However, in some instances we have observed destruction of TE cells before depletion

of thymocytes. Alternatively, cross-reactivity occurs between the HIV p19 and gp41 proteins and TE cell antigens such as HLA-DR (40, 41), such that an immune response mounted against HIV might target normal TE cells. However, this is unlikely to occur in the SCID-hu thymus. It is clear that the thymic microenvironment is a complex tissue requiring the intact function of thymocytes, TE cells, and even fibroblasts (30) for normal development, growth, and T cell maturation. The mechanism by which HIV disrupts this environment is an area of ongoing investigation.

In summary, infection of the human thymus in the SCID-hu mouse results in infection of both distinct thymocyte subsets and TE cells. Thymocyte depletion and TE cell degeneration occur. The depletion of thymocytes by HIV infection and, in particular, the ability of HIV to disrupt the TE cell supporting framework of the thymus, has broad implications for therapies aimed at reconstitution of the immune system in HIV-infected individuals.

Address correspondence to Sharilyn K. Stanley, Laboratory of Immunoregulation, National Institutes of Health, Building 10, Room 6A11, Bethesda, MD 20892.

References

1. Fauci, A.S. 1988. The human immunodeficiency virus: infectivity and mechanisms of pathogenesis. Science (Wash. DC). 239:617.

2. Schnittman, S.M., J.J. Greenhouse, M.C. Psallidopoulos, M. Baseler, N.P. Salzman, A.S. Fauci, and H.C. Lane. 1990. Increasing viral burden in CD4+ T cells from patients with human immunodeficiency virus (HIV) infection reflects rapidly progressive immunosuppression and clinical disease. Ann. Intern. Med. 113:438.

3. Lyerly, H.K., T.J. Matthews, A.J. Langlois, D.P. Bolognesi, and K.J. Weinhold. 1987. Human T-cell lymphotropic virus IIIB glycoprotein (gp120) bound to CD4 determinants on normal lymphocytes and expressed by infected cells serves as target for immune attack. Proc. Natl. Acad. Sci. USA. 84:4601.

4. Katz, J.D., P. Nishanian, R. Mitsuyasu, and B. Bonavida. 1988. Antibody-dependent cellular cytotoxicity (ADCC)–mediated destruction of human immunodeficiency virus (HIV)-coated CD4+ T lymphocytes by acquired immunodeficiency syndrome (AIDS) effector cells. J. Clin. Immunol. 8:453.

5. Groux, H., G. Torpier, D. Monte, Y. Mouton, A. Capron, and J.C. Ameisen. 1992. Activation-induced death by apoptosis in CD4+ T cells from human immunodeficiency virus-infected asymptomatic individuals. J. Exp. Med. 175:331.

6. Kennedy, J.R. 1992. Aids—an autoimmune model. Med. Hypotheses. 37:16.

7. Schnittman, S.M., S.M. Denning, J.J. Greenhouse, J.S. Justement, M. Baseler, J. Kurtzberg, B.F. Haynes, and A.S. Fauci. 1990. Evidence for susceptibility of intrathymic T-cell precursors and their progeny carrying T-cell antigen receptor phenotypes TCRαβ+ and TCRγδ+ to human immunodeficiency virus

infection: a mechanism for CD4+ (T4) lymphocyte depletion. Proc. Natl. Acad. Sci. USA. 87:7727.

8. De Rossi, A., M.L. Calabro, M. Panozzo, D. Bernardi, B. Caruso, G. Tridente, and L. Chieco-Bianchi. 1990. In vitro studies of HIV-1 infection in thymic lymphocytes: a putative role of the thymus in AIDS pathogenesis. AIDS Res. Hum. Retroviruses. 6:287.

9. Folks, T.M., S.W. Kessler, J.M. Orenstein, J.S. Justement, E.S. Jaffe, and A.S. Fauci. 1988. Infection and replication of HIV-1 in purified progenitor cells of normal human bone marrow. Science (Wash. DC). 242:919.

10. Stanley, S.K., S.W. Kessler, J.S. Justement, S.M. Schnittman, J.J. Greenhouse, C.C. Brown, L. Musongela, K. Musey, B. Kapita, and A.S. Fauci. 1992. CD34+ bone marrow cells are infected with HIV in a subset of seropositive individuals. J. Immunol. 149:689.

11. Namikawa, R., H. Kaneshima, M. Lieberman, I.L. Weissman, and J.M. McCune. 1988. Infection of the SCID-hu mouse by HIV-1. Science (Wash. DC). 242:1684.

12. Grody, W.W., S. Fligiel, and F. Naeim. 1985. Thymus involution in the acquired immunodeficiency syndrome. Am. J. Clin. Pathol. 84:85.

13. Seemayer, T.A., A.C. Laroche, P. Russo, R. Malebranche, E. Arnoux, J.M. Guerin, G. Pierre, J.M. Dupuy, J.G. Gartner, W.S. Lapp, et al. 1984. Precocious thymic involution manifest by epithelial injury in the acquired immune deficiency syndrome. Hum. Pathol. 15:469.

14. Schuurman, H.J., W.J.A. Krone, R. Broekhuizen, J.V. Baarlen, P. van Veen, A.L. Goldstein, J. Huber, and J. Goudsmit. 1989. The thymus in acquired immune deficiency syndrome: com-

parison with other types of immunodeficiency diseases, and presence of components of human immunodeficiency virus type 1. *Am. J. Pathol.* 134:1329.

15. Joshi, V.V., and J.M. Oleske. 1985. Pathologic appraisal of the thymus gland in acquired immunodeficiency syndrome in children. *Arch. Pathol. Lab. Med.* 109:142.

16. Papiernik, M., Y. Brossard, N. Mulliez, J. Roume, C. Brechot, F. Barin, A. Goudeau, J.F. Bach, C. Griscelli, R. Henrion, and R. Vazeux. 1992. Thymic abnormalities in fetuses aborted from human immunodeficiency virus type 1 seropositive women. *Pediatrics.* 89:297.

17. McCune, J.M., R. Namikawa, H. Kaneshima, L.D. Shultz, M. Lieberman, and I.L. Weissman. 1988. The SCID-hu mouse: murine model for the analysis of human hematolymphoid differentiation and function. *Science (Wash. DC).* 241:1632.

18. Namikawa, R., K. Weilbaecher, H. Kaneshima, E. Yee, and J.M. McCune. 1990. Long-term human hematopoiesis in the SCID-hu mouse. *J. Exp. Med.* 172:1055.

19. McCune, J., H. Kaneshima, J. Krowka, R. Namikawa, H. Outzen, B. Peault, L. Rabin, C.C. Shih, and E. Yee. 1991. The SCID-hu mouse: a small animal model for HIV infection and pathogenesis. *Annu. Rev. Immunol.* 9:399.

20. Krowka, J., S. Sarin, R. Namikawa, J.M. McCune, and H. Kaneshima. 1991. Characteristics of human lymphocytes in the peripheral blood of SCID-hu mice. *J. Immunol.* 146:3751.

21. Vandekerckhove, B.A.E., J.R. Krowka, J.M. McCune, J.E. deVries, H. Spits, and M.G. Roncarolo. 1991. Clonal analysis of the peripheral T cell compartment of the SCID-hu mouse. *J. Immunol.* 146:4173.

22. Koyanagi, Y., S. Miles, R.T. Mitsuyasu, J.E. Merrill, H.V. Vinters, and I.S.Y. Chen. 1987. Dual infection of the central nervous system by AIDS viruses with distinct cellular tropisms. *Science (Wash. DC).* 23:819.

23. Schnittman, S.M., M.C. Psallidopoulos, H.C. Lane, L. Thompson, M. Baseler, F. Massari, C.H. Fox, N.P. Salzman, and A.S. Fauci. 1989. The reservoir for HIV-1 in human peripheral blood is a T cell that maintains expression of CD4. *Science (Wash. DC).* 245:305.

24. Clouse, K.A., D. Powell, I. Washington, G. Poli, K. Strebel, W. Farrar, P. Barstad, J. Kovacs, A.S. Fauci, and T.M. Folks. 1989. Monokine regulation of human immunodeficiency virus-1 expression in a chronically infected human T cell clone. *J. Immunol.* 142:431.

25. Graziosi, C., G. Pantaleo, and A.S. Fauci. 1992. Detection of HIV DNA and RNA by PCR. *Curr. Protocols Immunol.* Suppl. 5:12.6.5.

26. Folks, T.M., D. Powell, M. Lightfoote, S. Koenig, A.S. Fauci, S. Benn, A. Rabson, D. Daugherty, H.E. Gendelman, M.D. Hoggan, et al. 1986. Biological and biochemical characterization of a cloned Leu-3⁻ cell surviving infection with the acquired immune deficiency syndrome retrovirus. *J. Exp. Med.* 164:280.

27. Fox, C.H., and M. Cottler-Fox. 1993. In situ hybridization for detection of HIV in cells and tissues. *Curr. Protocols Immunol.* Suppl. 6:12.8.1.

28. Spiegel, H., H. Herbst, G. Niedobitek, H.D. Foss, and H.

Stein. 1992. Follicular dendritic cells are a major reservoir for human immunodeficiency virus type 1 in lymphoid tissues facilitating infection of CD4⁺ T-helper cells. *Am. J. Pathol.* 140:15.

29. Orenstein, J.M., and F. Jannotta. 1988. Human immunodeficiency virus and papovavirus infections in acquired immunodeficiency syndrome. *Hum. Pathol.* 19:350.

30. Haynes, B.F., R.M. Scearce, D.F. Lobach, and L.L. Hensley. 1984. Phenotypic characterization and ontogeny of mesodermal-derived and endocrine epithelial components of the human thymic microenvironment. *J. Exp. Med.* 159:1149.

31. Fox, C.H., K. Tener-Racz, P. Racz, A. Firpo, P.A. Pizzo, and A.S. Fauci. 1991. Lymphoid germinal centers are reservoirs of human immunodeficiency virus-type 1 RNA. *J. Infect. Dis.* 164:1051.

32. Pantaleo, G., C. Graziosi, J.F. Demarest, L. Butini, M. Montroni, C.H. Fox, J.M. Orenstein, D.P. Kotler, and A.S. Fauci. 1993. HIV infection is active and progressive in lymphoid tissue during the clinically latent stage of disease. *Nature (Lond.).* 362:355.

33. Bonyhadi, M.L., J. Kaneshima, and J.M. McCune. 1992. Effects of HIV infection in human fetal thymus in the SCID-hu mouse. *J. Cell. Biochem.* 16E:45.

33a. Aldrovandi, G.M., G. Feuer, L. Gao, B. Jamieson, M. Kristeva, I.S.Y. Chen, and J.A. Zack. 1993. The SCID-hu mouse as a model for HIV-1 infection. *Nature (Lond.)* 363:732.

34. York-Higgins, D., C. Cheng-Mayer, D. Bauer, J.A. Levy, and D. Dina. 1990. Human immunodeficiency virus type 1 cellular host range, replication, cytopathicity are linked to the envelope region of the viral genome. *J. Virol.* 64:4016.

35. Koga, Y., M. Sasaki, H. Yoshida, H. Wigzell, G. Kimura, and K. Nomoto. 1990. Cytopathic effect determined by the amount of CD4 molecules in human cell lines expressing envelope glycoprotein of HIV. *J. Immunol.* 144:94.

36. De Maria, A., G. Pantaleo, S.M. Schnittman, J.J. Greenhouse, M. Baseler, J.M. Orenstein, and A.S. Fauci. 1991. Infection of CD8⁺ T lymphocytes with HIV. *J. Immunol.* 146:2220.

37. Numazaki, K., X.Q. Bai, H. Goldman, I. Wong, B. Spira, and M.A. Wainberg. 1989. Infection of cultured human thymic epithelial cells by human immunodeficiency virus. *Clin. Immunol. Immunopathol.* 51:185.

38. Denning, S.M., D.T. Tuck, K.H. Singer, and B.F. Haynes. 1987. Human thymic epithelial cells function as accessory cells for autologous mature thymocyte activation. *J. Immunol.* 138:680.

39. van de Wijngaert, F.P., M.D. Kendall, H.J. Schuurman, L.H.P.M. Rademakers, and L. Kater. 1984. Heterogeneity of epithelial cells in the human thymus: an ultrastructural study. *Cell Tissue Res.* 237:227.

40. Parravicini, C.L., D. Klatzmann, P. Jaffray, G. Costanzi, and J.C. Gluckman. 1988. Monoclonal antibodies to the human immunodeficiency virus p18 protein cross-react with normal human tissues. *AIDS (Phila.).* 2:171.

41. Golding, H., F.A. Robey, F.T. Gates III, W. Linder, P.R. Beining, T. Hoffman, and B. Golding. 1988. Identification of homologous regions in human immunodeficiency virus I gp41 and human MHC class II β1 domain. *J. Exp. Med.* 167:914.